JOURNAL OF THE KOREAN ASTRONOMICAL SOCIETY
38: 295 ~ 298, 2005

A METHOD FOR DETERMINING MAGNETIC HELICITY OF SOLAR ACTIVE REGIONS FROM SOHO/MDI MAGNETOGRAMS

JONGCHUL CHAE AND HYEWON JEONG
Astronomy Program, School of Earth and Environmental Science, Seoul National University, Seoul 151-742, Korea
E-mail: chae@astro.snu.ac.kr
(Received February 1, 2005; Accepted March 15, 2005)

ABSTRACT

Recently a big progress has been made on the measurements of magnetic helicity of solar active regions based on photospheric magnetograms . In this paper, we present the details of Chae's method of determining the rate of helicity transfer using line-of-sight magnetograms such as taken by SOHO/MDI. The method is specifically applied to full-disk magnetograms that are routinely taken at 96-minute cadence.

Key words : sun: magnetic field — sun: photosphere — sun: active regions

I. INTRODUCTION

Magnetic helicity has become an important concept in understanding the behavior of magnetic flux systems on the Sun not only because it is a well-conserved physical parameter, but also because it is now a measurable quantity. Currently the photosphere is the only atmospheric level at which we can reasonably measure solar magnetic fields. Chae et al. (2004) gave a brief review of different studies on measuring magnetic helicity using photospheric magnetograms, so we don't feel the need to repeat it here. They also demonstrated that Chae's method (Chae 2001) originally proposed for vertical magnetic fields may be generalized to inclined magnetic fields based on the relation

$$dH/dt = -\oint 2(\boldsymbol{u}\cdot\boldsymbol{A}_p)B_n\,dS, \qquad (1)$$

where $\boldsymbol{A}_p$ is the vector potential of potential field wholly specified by the normal field component B_n, and $\boldsymbol{u}$ represents the horizontal velocity component of the apparent motion of field line footpoints.

Chae's method uses a time sequence of line-of-sight magnetograms as a basic input. The recent version given by the Chae et al. (2004) made it possible to trace the magnetic helicity of a large number of solar active regions for several days in each rotation period, using SOHO/MDI full-disk magnetograms that are routinely taken at 96-minute cadence. This paper is an extension of Chae et al. (2004), and deals with the details of the procedures in the method. For illustration, we use the same data for the active region AR 10365 as used by Chae et al.(2004).

Proceedings of *the 6th East Asian Meeting of Astronomy*, held at Seoul National University, Korea, from October 18-22, 2004.

II. METHOD

(a) Selecting the Data Files

The basic input data are the list of FITS files containing magnetograms and the information necessary to specify the active region of interest. We define a reference point inside the active region, usually at its center, and assume that it rotates at a standard differential rotation rate (Howard et al. 1990). The image plane position of the reference point (X_r, Y_r) at the reference time t_r should be given as an input. Note that the capitals X and Y represent the SOHO image plane coordinates in which the origin is at the disk center, X-direction is to the solar west and the Y-direction to the north. The coordinates are measured in unit of arc seconds.

To reduce troubles arising from the geometrical projection effect (Chae et al. 2001), we select only the data files containing magnetograms that were taken while the reference point was not far from the disk center. This is achieved by requiring that the image plane distance d from the disk center be smaller than a predefined critical value d_c. If one takes a too small value of d_c, the data are little subject to the geometrical projection effect, but the number of data files to be used may be too small. Therefore a compromise has to be made for a suitable choice of d_c between the two different needs. We usually adopt $d_c = 0.6R$ where R is the angular radius of the solar disk. With this value the heliocentric angle $\psi = \sin^{-1}(d_c/R)$ of the active region remains less than 37°, and it is possible to trace the active region without interruption for about five days per each rotation.

The parameters (X_r, Y_r) at t_r are used to determine not only the heliographic latitude B_r and longitude L_r of the reference point at the reference time t_r, but also the SOHO coordinates (X_k, Y_k) at the specified observing times t_k $(k = 1, ..., N)$ of the data files. For coordinate transformation we make use of the IDL pro-

grams ARCMIN2HEL and HEL2ARCMIN in the SolarSoft (Freeland and Handy 1998). Given the latitude and longitude of the disk center which are functions of time, ARCMIN2HEL converts the SOHO coordinates into the heliographic coordinates, and HEL2ARCMIN does the reverse process.

We use ARCMIN2HEL to convert the SOHO image plane coordinates (X_r, Y_r) into heliographic coordinates (B_r, L_r). Since the reference point has been assumed to rotate at a rate that may be different from the Carrington rotation rate (13.1988°/day), L may change with time. Therefore, L_k at every t_k should be determined from L_r and $t_k - t_r$ taking into account the difference between Howard et al.'s (1990) rotation rate and the Carrington rotation rate. On the other hand, B_k remains the same as B_r without change. With the help of the IDL program HEL2ARCMIN, the heliographic coordinates B_k and L_k are then converted the SOHO image plane coordinates (X_k, Y_k) of the reference point at t_k. The image plane distance of the reference point from the disk center at t_k is given by $d = \sqrt{X_k^2 + Y_k^2}$.

(b) Preparing the Data Cube

The magnetograms contained in the selected data files are used for the construction of a data cube. Each slice of the data cube is a two-dimensional array representing a map of vertical component of photospheric magnetic field at a specific time. The indices of the array correspond to local Cartesian x and y coordinates defined on the tangential plane of the solar surface of which contact point is the reference point. The z-direction hence coincides with the normal direction at the reference point. The x-direction is set to the local west, and the y-direction is set to the local north. Thus, by definition, it always follows $x = y = 0$ at the reference point. Note that the x and y coordinates are identical to the SOHO coordinates if the reference point is on the disk center. As a matter of fact, our mapping is intended to reconstruct the magnetograms in the way they look as if the active region of our interest is always on the disk center.

The specification of the grid size δ, the east and west boundaries x_e, x_w and the south and north boundaries y_s, y_n defines the grid system

$$x_i = x_e + i\delta \quad \text{where } i = 0, 1, .., (x_w - x_e)/\delta, \quad (2)$$

$$y_j = y_s + j\delta \quad \text{where } j = 0, 1, .., (y_n - y_s)/\delta \ , \quad (3)$$

We typically choose $\delta = 1''$, about half the pixel size of MDI full-disk magnetograms, which means that our reconstruction or re-mapping of magnetograms is implementing sub-pixelization. The re-mapping of the magnetogram at a specific observing time t_k requires the the transformation of the local coordinates of the two-dimensional grids (x_i, y_j) to the corresponding SOHO coordinates (X_{ij}^k, Y_{ij}^k). This transformation is carried out in two steps.

Firstly, the conversion of the local coordinates (x_i, y_j) into the heliographic coordinates (B_{ij}^k, L_{ij}^k) is carried out with ARCMIN2HEL by setting the latitude and longitude of the disk center to those of the reference point (B_k, L_k) at the observing time t_k. Note (B_k, L_k) should be determined first in the way described above. Then the conversion from (B_{ij}^k, L_{ij}^k) to the SOHO coordinates (X_{ij}^k, Y_{ij}^k) are performed using HEL2ARCMIN with the latitude and longitude of the disk center being set to the true ones at t_k.

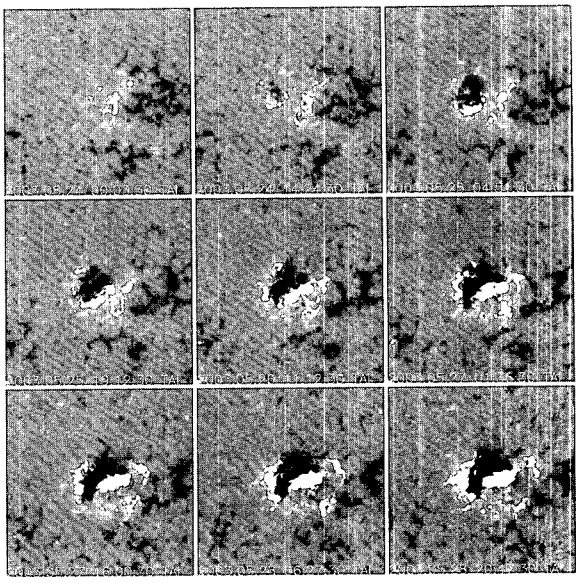

Fig. 1.— Some of magnetograms in a data cube.

A magnetogram contained in a FITS file is a two-dimensional array of the line-of-sight magnetic field B_l where the SOHO coordinates of the array grids are known from the information on the header. Then the line-of-sight field at every position specified by the SOHO coordinates (X_{ij}^k, Y_{ij}^k) is determined based on the two-dimensional linear interpolation. Finally the component B_n should be determined. Since the line-of-sight field B_l is the only field component that can be measured by SOHO/MDI, the best we can do is to assume that the magnetic field on the solar photosphere is normal to the solar surface. Then it follows

$$B_n = \frac{B_l}{\cos\psi} = \frac{B_l}{\sqrt{1 - (X^2 + Y^2)/R^2}}, \quad (4)$$

where ψ is the heliocentric angle of the point of interest. This assumption is a good approximation either near the disk center even if magnetic fields are inclined, or much away from the disk center where the fields are normal to the surface. It's validity, however, may weaken in the case of inclined magnetic fields at regions that are much away from the disk center and hence have large values of ψ. The detailed discussion on this aspect was given in the Appendix of Chae et al. (2001). This may introduce some uncertainties in the measured helicity rate, and may be the major weakness

of our method.

The final outcome of the re-mapping procedure is the three-dimensional array $B^k_{n,ij}$ or a data cube where i and j represent the spatial indices and k the time index. Note that the data cube represents a time sequence of magnetograms that are spatially aligned with one another. The spatial alignment is done by the successive re-mapping which automatically tracks the reference point using the standard differential rotation rate. This approach as adopted by Chae et al. (2004) is a little different from the initial approach used by Chae (2001) and Chae et al. (2001). In this earlier approach the re-mapping was realized by tracking every grid in the region of interest individually taking into account the differential rotation at every grid. Thus the effect of the differential rotation was automatically subtracted from the velocity field which was determined from the data cube. This approach, however, may cause a distortion in the magnetograms in the data cube unless the individual points in the region rotate at the specified differential rotation rate especially when the time span is long. This is why we are adopting the new approach in which only the reference point is tracked using the information of the differential rotation rate. Figure 1 illustrates a data cube constructed in the method described above.

(c) Calculating the Vector Potential

The vector potential $\boldsymbol{A}_p$ should satisfy the equations

$$\nabla \times \boldsymbol{A}_p \cdot \boldsymbol{n} = B_n \quad \nabla \cdot \boldsymbol{A}_p = 0 \quad \boldsymbol{A}_p \cdot \boldsymbol{n} = 0, \qquad (5)$$

the Fourier solution which was given by Chae (2001). According to our experience, the Fourier solution is usually satisfying unless the region of interest is too close to the boundary of the spatial domain of the Fourier transform. We usually take the spatial domain big enough to contain a big neighboring quiet area as well as the active region itself.

Given the three-dimensional array $B^k_{n,ij}$ as an input, we obtain two three-dimensional arrays $A^k_{px,ij}$ and $A^k_{py,ij}$ as an output by repeating the calculation of the Fourier solution for every k.

(d) Calculating the Velocity Field

The velocity $\boldsymbol{u}$ at a point is determined from the horizontal displacement of the pattern of B_n in the local area surrounding the point. It describes not the true plasma motion, but the apparent motion of the fieldline footpoints. Chae (2001) used the technique of the local correlation tracking (LCT, November and Simon 1988) to find out the horizontal displacement. The two important parameters in this method are the full width at half maximum (FWHM) of the window function defining the extent of the local area, and the time interval Δt between two successive frames to be compared. The effects of these two parameters were studied in detail by Chae et al. (2004). For the 96-minute cadence, full-disk magnetograms, we typically choose a FWHM of $10''$ and $\Delta t = 96$ minutes.

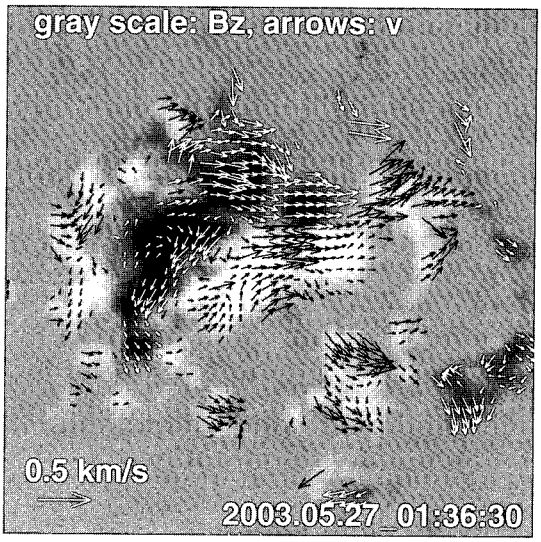

Fig. 2.— Velocity field plotted as arrows. The gray scale represents the normal field distribution.

Constructing the velocity field by applying LCT is a time-consuming work, because the velocity should be determined at a large number of points point by point. The number of points is about $400 \times 400 = 160000$ for a typical region of $400'' \times 400''$ size when sampled with $\delta = 1''$. To save the computing time, we reduce the number of the data points where the velocity should be determined. For this we devise a new grid system

$$x'_l = x'_e + l\delta' \text{ where } l = 0, 1, .., (x'_w - x'_e)/\delta', \quad (6)$$
$$y'_m = y'_s + m\delta' \text{ where } m = 0, 1, .., (y'_n - y'_s)/\delta' \quad (7)$$

with the new parameters x'_e, x'_w, y'_s, y'_n, and δ' satisfying the condtions

$$x'_e \geq x_e,\ x'_w \leq x_w,\ y'_s \geq y_s\ y'_n \leq y_n,\ \delta' \geq \delta, \qquad (8)$$

If we choose appropriate parameter values satisfying, for example, $x'_w - x'_e = y'_s - y'_n = 300''$ and $\delta' = 4\delta = 4''$, the number of data points becomes reduced to 5625, a much smaller number than 160000. This reduction in the number of data points is mainly due to the increase of the grid size, or the super-pixelization. Note that this size of the macropixel is about twice the original pixel size of MDI full-disk magnetograms and less than half of the FWHM of the window function. Therefore, it appears a reasonable value, not being too big.

Using this grid system, the velocity field is expressed as two three-dimensional arrays $u^{k+1/2}_{x,lm}$ and $u^{k+1/2}_{y,lm}$ where the index $k + 1/2$ means that the velocity field is determined at the middle of the two instants represented by the indices k and $k + 1$. It should be emphasized that $u^{k+1/2}_{x,lm}$ and $u^{k+1/2}_{y,lm}$ are determined from $B^k_{n,ij}$

which has a grid size of $\delta = 1''$. Since a circular area specified by a diameter of $10''$ will contain a sufficiently large number of pixels (about 80), LCT is not subject to the the low sampling problem.

A couple of more things need to be mentioned in regard to the velocity measurement. Firstly, the application of the LCT is restricted to the macropixels only where $|B_n|$ is greater than a threshold B_c of, for example, 5 G. At other macropixels not satisfying this condition, the velocity is set to zero without applying the LCT. This further reduces the number of data points roughly by a factor of two. In addition, even if the LCT is applied, the velocity is set to zero again if the cross correlation coefficient is too small, for example, less than 0.8. This is because the velocity field obtained from LCT might have physically meaningless, or even harmful values, when the cross relation is low.

Figure 2 shows the velocity field at an instant. Note that the velocity was determined at the macropixels, but for visualization the velocity arrows are drawn at every two macropixels and the zero velocity vectors have been suppressed.

(e) Calculating the Helicity Rate

Once the velocity arrays $u_{x,lm}^{k+1/2}$ and $u_{y,lm}^{k+1/2}$ are found, the magnetic field and the vector potential also are re-gridded in this new grid system using the linear interpolation technique, being expressed as $B_{n,lm}^{k+1/2}$ and $A_{px,lm}^{k+1/2}$, $A_{py,lm}^{k+1/2}$.

Then the rate dH/dt of the helicity transfer through the photosphere is given by

$$(dH/dt)^k = -2(\delta')^2 \sum_{l,m} (u_{x,lm}^{k+1/2} A_{px,lm}^{k+1/2} + u_{y,lm}^{k+1/2} A_{py,lm}^{k+1/2}) B_{n,lm}^{k+1/2}, \quad (9)$$

and the accumulated amount of helicity transfer ΔH is given by

$$(\Delta H)^k = \sum_{k'=1}^{k'=k} (dH/dt)^{k'} (t_{k'+1} - t_{k'}), \quad (10)$$

Figure 3 shows the rate of helicity transfer $(dH/dt)^k$ plotted as a function of time t_k, and Figure 4, the accumulated amount of helicity change $(\Delta H)^k$. The accumulated helicity increased with time as the total flux did. A careful examination, however, reveals that the amount of helicity transfer is not proportional to the amount of the total flux. This may have some interesting physical implications that may be worth further investigations.

III. CONCLUSION

We have presented the details of the method of determining magnetic helicity of solar active regions

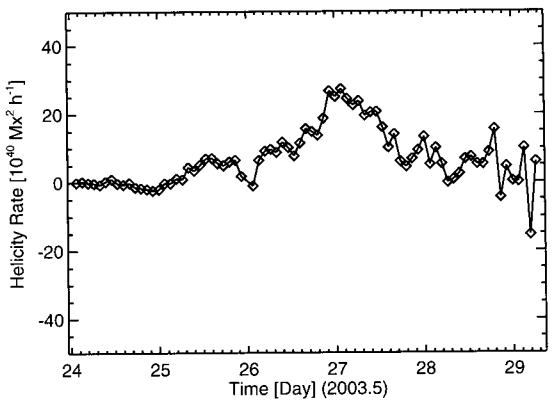

Fig. 3.— Helicity rate as a function of time

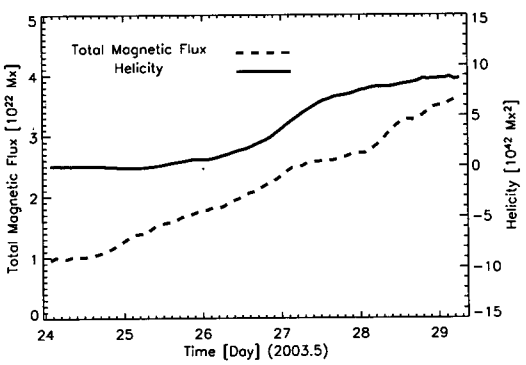

Fig. 4.— Total flux (absolute sum of positive and negative flux) and helicity as functions of time

(Chae et al. 2004) especially for the case making use of the routinely available magnetograms in the MDI data archive. The method will serve for the investigation of the magnetic helicity history in a large number of active regions.

ACKNOWLEDGEMENTS

This work was supported by the New Faculty Grant of Seoul National University.

REFERENCES

Chae, J. 2001, ApJ Letters, 560, L95

Chae, J., Wang, H., Qiu, J., Goode, P. R., Strous, L., Yun, H. S. 2001, ApJ, 560, 476

Chae, J., Moon, Y.-J., Park, Y.-D. 2004, Solar Phys., in press

Freeland, S. L., Handy, B. N. 1998, Solar Phys., 182, 497q

Howard, R. F., Harvey, J. W., Forgach, S. 1990, Solar Phys., 130, 295

November, L. J., Simon, G. W. 1988, ApJ, 333, 427